Compton Scattering and Nonforward Parton Distributions

A.V. RADYUSHKIN

Physics Department, Old Dominion University,
Norfolk, VA 23529, USA
and
Jefferson Lab,
Newport News,VA 23606, USA

Compton amplitudes. Compton scattering (see Fig.1) in its various versions provides a unique tool for studying many aspects of hadronic structure probing it by two electromagnetic currents. In QCD, the photons couple to quarks of a hadron through a vertex which is pointlike in the simplest approximation. However, in the soft regime, strong interactions produce large corrections uncalculable within the perturbative QCD framework. To take advantage of the basic pointlike structure of the photon-quark coupling, one should choose a specific kinematics securing the short-distance dominance by the presence of a large momentum transfer.
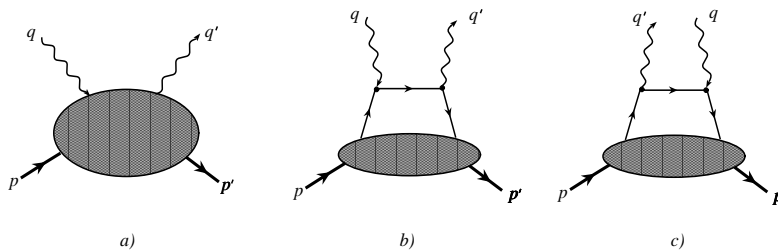

FIG. 1. *a)* General Compton amplitude; *b)* s-channel handbag diagram; *c)* u-channel handbag diagram.

Deep inelastic scattering. Virtual forward Compton amplitude whose imaginary part gives structure functions of deep inelastic scattering is the most well-known case of a short-distance-dominated Compton amplitude. In this case, the "final" photon has momentum $q' = q$ coinciding with that of the initial one. The momenta p, p' of the initial and final hadrons also

1

coincide. The short-distance dominance is guaranteed by high virtuality of the photons: $-q^2 \equiv Q^2 > 1$ GeV^2. Moreover, the total cm energy of the photon-hadron system $s = (p + q)^2$ should be above resonance region, and the Bjorken ratio $x_{Bj} = Q^2/2(pq)$ is finite. In the large-Q^2 limit, the dominant contribution is given by the handbag diagram in which the perturbatively calculable hard quark propagator is convoluted with parton distribution functions $f_a(x)$ ($a = u, d, s, \ldots$) which describe/parametrize nonperturbative information about hadronic structure.

Deeply virtual Compton scattering (DVCS). In this case, the initial photon is highly virtual while the final photon is real. The momentum transfer t should be as small as possible [1]. Large virtuality of the initial photon is sufficient for making the handbag diagram dominant [2–4]. Again, the leading term is given by a convolution of the hard quark propagator and a nonperturbative function $\mathcal{F}_\zeta(X; t)$ (*nonforward parton distribution** [2]) describing long-distance dynamics. In addition to the "usual" parton variable X giving the fraction Xp^+ of the "+" component ($p^+ = p^0 + p^3$) of the initial hadron momentum p carried by the quark, it also depends on the invariant momentum transfer $t = (p' - p)^2$, and the "skewedness" parameter $\zeta = r^+/p^+$ (where $r \equiv p - p'$) specifying the longitudinal momentum asymmetry of the nonforward matrix element. This asymmetry appears because it is impossible to convert a highly virtual initial photon into a real final photon without a longitudinal momentum transfer (the longitudinal direction is specified by p and q). For the DVCS amplitude, the skewedness parameter ζ coincides with the Bjorken variable $x_{Bj}{}^\dagger$.

Wide-angle real Compton scattering (WACS). With both photons real, it is not sufficient to have large photon energy to ensure short-distance dominance: large-s, small-t region is dominated by Regge contributions for which no simple parton description is possible. Hence, having large $|t| > 1$GeV^2 is a necessary condition for revealing short-distance dynamics. The leading-order contribution in the large-s, large-t limit is again given by

---

*X.Ji introduced originally *off-forward parton distributions* $H(x, \xi; t)$ [1], with parton momentum being xP, where $P = (p + p')/2$.

†In Ji's approach [1], the skewedness is characterized by the parameter $\xi = x_{Bj}/(2 - x_{Bj})$.

handbag diagrams [5] in which hard quark propagator is convoluted with the nonforward parton distributions $\mathcal{F}^a_{\zeta=0}(X;t)$. Since the initial photon is real, it can be converted into the final one by a purely transverse momentum transfer, so the skewedness parameter ζ vanishes.

Hybrid nature of nonforward parton distributions (NFPD's). The NFPD's $\mathcal{F}^a_\zeta(X;t)$ look like form factors with respect to t and like parton distributions with respect to X. Due to the spectral property $0 \leq X \leq 1$, both the parton going out of the hadron and the spectators carry positive fractions of the initial hadron momentum (parton picture implies a frame where the hadron moves fast).
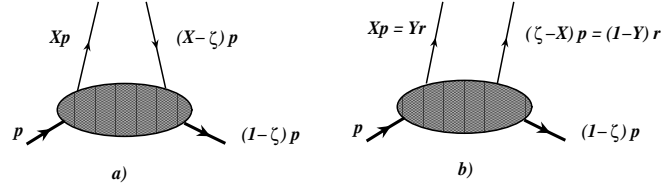

FIG. 2. Nonforward parton distribution in two regions: *a*) $X > \zeta$ and *b*) $X < \zeta$.

Unlike in the forward case, the "returning" parton carries a smaller fraction $X' \equiv X - \zeta$ of the original hadron momentum p. Since $0 < \zeta < 1$, the fraction X' can be either positive or negative, i.e., each NFPD has two components. In the region $\zeta < X < 1$ (Fig. 2*a*), the function $\mathcal{F}_\zeta(X)$ describes a parton going out of the hadron with a positive fraction Xp of the original hadron momentum and then coming back into the hadron with a changed (but still positive) fraction $(X - \zeta)p$. In the region $0 < X < \zeta$ (Fig. 2*b*), the "returning" parton has a negative fraction $(X - \zeta)$ of the light-cone momentum p. Hence, it is more appropriate to treat it as a parton going out of the hadron and propagating along with the original parton. Writing X as $X = Y\zeta$, we see that both partons carry now positive fractions $Y\zeta p \equiv Yr$ and $(1 - Y)r$ of the momentum transfer r. In the region $X = Y\zeta < \zeta$, NFPD's look like distribution amplitudes (wave functions) $\Psi_\zeta(Y) = \mathcal{F}_\zeta(\zeta Y)$ characterizing the probability amplitude for the initial hadron with momentum p to split into the final hadron with momentum $(1 - \zeta)p$ and a two-parton state with total momentum $r = \zeta p$ shared by the

partons in fractions Yr and $(1-Y)r$ (see Fig.2).

Possible shape of nonforward distributions $\mathcal{F}_\zeta(X)$ is illustrated in Fig.3. A characteristic feature of each curve is a maximum located close to the relevant border point $X = \zeta$ and slightly shifted to the left from it[‡]. The curves shown there were obtained in a model [6] based on so-called double distributions (DD's) $F(x, y; t)$ which provide an alternative parametrization [2] of nonforward matrix elements, in which the parton momentum is written as $xp + yr$. DD's behave like parton densities wrt x and like distribution amplitudes wrt y.
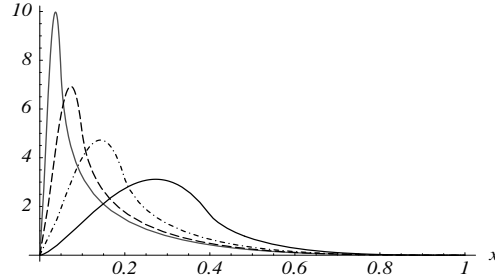

FIG. 3. Nonforward parton distributions $\mathcal{F}_\zeta(X)$ for different values of the skewedness $\zeta = 0.05$ (thin line), $\zeta = 0.1$ (dashed line), $\zeta = 0.2$ (dash-dotted line) and $\zeta = 0.4$ (full line) in the "valence quark oriented" model of ref. [6].

Formally, nonforward parton distributions are definined through matrix elements of light-cone operators

$$\langle p', s' \mid \bar{\psi}_a(0)\hat{z}E(0, z; A)\psi_a(z) \mid p, s \rangle|_{z^2=0} \tag{1}$$
$$= \bar{u}(p', s')\hat{z}u(p, s) \int_0^1 \left(e^{-iX(pz)}\mathcal{F}_\zeta^a(X; t) - e^{i(X-\zeta)(pz)}\mathcal{F}_\zeta^{\bar{a}}(X; t) \right) dX$$

[‡]More exotic results with rapid variation of NFPD's in the region $X \sim \zeta$ were obtained in the chiral soliton model [7].

$$+ \bar{u}(p', s') \frac{\hat{z}\hat{r} - \hat{r}\hat{z}}{4M} u(p, s) \int_0^1 \left(e^{-iX(pz)} \mathcal{K}_\zeta^a(X; t) - e^{i(X - \zeta)(pz)} \mathcal{K}_\zeta^{\bar{a}}(X; t) \right) dX.$$

Here $E(0, z; A)$ is the straight-line gauge link, M is the nucleon mass, s, s' specify the nucleon polarization and $\bar{u}(p', s'), u(p, s)$ are Dirac spinors. We use the "hat" convention $\hat{z} \equiv z^\mu \gamma_\mu$.

Using this definition, one can relate NFPD's to simpler functions which have been already studied experimentally. For instance, if $p = p'$, the matrix element coincides with the forward one defining usual parton distribution functions. This results in

$$\mathcal{F}_{\zeta=0}^a(X, t = 0) = f_a(X) \, ; \; \mathcal{F}_{\zeta=0}^g(X, t = 0) = X f_g(X).$$

Taking $z \to 0$, we see that integrating $\mathcal{F}_\zeta(X, t)$ over X one obtains hadronic form factors:

$$\sum_a e_a \int_0^1 \left[\mathcal{F}_\zeta^a(X; t) - \mathcal{F}_\zeta^{\bar{a}}(X; t) \right] dX = F_1(t) \, ,$$

where e_a is the electric charge of the relevant quark. The second type of distributions $\mathcal{K}_\zeta^a(X; t)$ present in Eq.(1) correspond to hadron helicity flip in the nonforward matrix element. They are related to the $F_2(t)$ form factor. Note, that the $\mathcal{K}$ functions are accompanied by the r factor in the above parametrization of the nonforward matrix element. Hence, they are invisible in deep inelastic scattering and other inclusive processes described by exactly forward $r = 0$ matrix elements. However, the $t = 0, \zeta = 0$ limit of the $\mathcal{K}$ distributions $\mathcal{K}_{\zeta=0}^a(X; t = 0) \equiv k_a(X)$ exists. In particular, the integral

$$\sum_a e_a \int_0^1 \left[k_a(X) - k_{\bar{a}}(X) \right] dX = \kappa_p$$

gives the proton anomalous magnetic moment. The X-moment of the flavor-singlet combination $k_a(X) + k_{\bar{a}}(X)$ contributes to the orbital momentum contribution to the proton spin [1]. Furthermore, there are also parton-helicity sensitive nonforward distributions $\mathcal{G}_\zeta^a(X; t)$ and $\mathcal{P}_\zeta^a(X; t)$. The first one reduces to the usual spin-dependent densities $\Delta f_a(x)$ in the $r = 0$ limit and gives the axial form factor $F_A(t)$ after the X-integration. The second one is similarly related to the pseudoscalar form factor $F_P(t)$.

Deeply virtual Compton scattering. In the lowest order, the DVCS amplitude $T^{\mu\nu}(p,q,q')$ is given by two handbag diagrams. In particular, the invariant amplitude containing the $\mathcal{F}$ functions is given by

$$T_F(p,q,q') = \sum_a e_a^2 \int_0^1 \left[\frac{1}{X - \zeta + i\epsilon} + \frac{1}{X - i\epsilon} \right] \mathcal{F}_\zeta^{a+\bar{a}}(X;t)\, dX \,. \qquad (2)$$

An important feature of the DVCS amplitude is that for large Q^2 and fixed t it depends only on the ratio $Q^2/2(pq) \equiv x_{Bj} = \zeta$: DVCS is an *exclusive* process exhibiting the Bjorken scaling.

One may ask which Q^2 are large enough to ensure the dominance of the lowest-twist handbag contribution. In DIS, approximate Bjorken scaling starts at $Q^2 \sim 2\,\mathrm{GeV}^2$. Another example is given by the exclusive process $\gamma(q_1)\gamma^*(q_2) \to \pi^0$ studied on $e^+ e^-$ colliders. If one of the photons is highly virtual $q_1^2 = -Q^2$ while another is (almost) real $q_2^2 \sim 0$, the process is kinematically similar to DVCS. In the leading order, the $F_{\gamma\gamma^*\pi^0}(Q^2)$ transition form factor is given by a handbag diagram again. The recent measurements by CLEO [8] show that the pQCD prediction $F_{\gamma\gamma^*\pi^0}(Q^2) \sim 1/Q^2$ again works starting from $Q^2 \sim 2\,\mathrm{GeV}^2$. The $\gamma\gamma^*\pi^0$ vertex (for a virtual pion) can be also measured on a fixed-target machine like CEBAF in which case it is just a part of the DVCS amplitude corresponding to the 4th nonforward distribution $\mathcal{P}_\zeta(X,t)$ (which is related to the pseudoscalar form factor $G_P(t)$ of the nucleon). Hence, CLEO data give an evidence that DVCS may be handbag-dominated for Q^2 as low as $2\,\mathrm{GeV}^2$.

The main problem for studying DVCS is the contamination by the Bethe-Heitler process in which the final photon is emitted from the initial or final electron. The Bethe-Heitler amplitude is enhanced at small t. On the other hand, the virtual photon flux for fixed Q^2 and x_{Bj} increases when the electron beam energy increases. Hence, the energy upgrade would make the DVCS studies at Jefferson Lab more feasible. Experimental aspects of virtual Compton scattering studies at Jefferson Lab were discussed at this workshop in the talk by C.E. Hyde-Wright [9].

The nonforward parton distributions can be also measured in hard meson electroproduction processes [2,10–12]. The leading-twist pQCD contribution in this case involves a one-gluon exchange, which means that the hard subprocess is suppressed by $\alpha_s/\pi \sim 0.1$ factor. The competing soft mechanism corresponds to a triple overlap of hadronic wave functions and has a relative suppression M^2/Q^2 by a power of Q^2, with $M^2 \sim 1$ GeV^2 being a

characteristic hadronic scale. Hence, to clearly see the one-gluon-exchange signal one needs Q^2 above $10\,\mathrm{GeV}^2$. Numerical pQCD-based estimates and comparison of DVCS and hard meson electroproduction cross sections [12] were presented at this workshop by M. Guidal [13].

Wide-angle real Compton scattering. At moderately large $s, |t|, |u| \lesssim 10$ GeV^2, the leading-order contribution to WACS amplitude is given by the s- and u-channel handbag diagrams with hard quark propagators $(x\hat{P} + \hat{Q})/xs$ and $(x\hat{P} - \hat{Q})/xs$, respectively, where $P = (p + p')/2, Q = (q + q')/2$. Since there is no skewedness, one deals with the functions $\mathcal{F}^a(x, t) \equiv \mathcal{F}^a_{\zeta=0}(x; t)$ and their $\mathcal{K}, \mathcal{G}, \mathcal{P}$ analogs. The *nonforward parton densities* (ND's) $\mathcal{F}^a(x, t)$ are the simplest hybrids of parton densities and hadronic form factors. They are related to the usual parton densities by $\mathcal{F}^a(x, t = 0) = f^a(x)$ and to form factors by

$$\sum_a e_a \int_0^1 \left[\mathcal{F}^a(x; t) - \mathcal{F}^{\bar{a}}(x; t) \right] \, dX = F_1(t) . \tag{3}$$

These relations are trivially satisfied by the factorized ansatz $\mathcal{F}^a_{val}(x; t) = f^a_{val}(x)F_1(t)$ (here $\mathcal{F}^a_{val}(x; t) \equiv \mathcal{F}^a(x; t) - \mathcal{F}^{\bar{a}}(x; t)$). However, explicit calculations within the light-cone formalism suggest a more complicated interplay between the x- and t-behavior of ND's. In particular, assuming a relativistic Gaussian dependence $\exp[-k_\perp^2/2x\bar{x}\lambda^2]$ ($\bar{x} \equiv 1 - x$) of the hadronic blob on the transverse momentum $k_\perp$, gives the model [5]

$$\mathcal{F}^a(x, t) = f^a(x)e^{\bar{x}t/4x\lambda^2} = \frac{f_a(x)}{\pi x\bar{x}\lambda^2} \int e^{-(k_\perp^2 + (k_\perp + \bar{x}r_\perp)^2)/2x\bar{x}\lambda^2} d^2k_\perp . \tag{4}$$

The functions $f_a(x)$ here are the usual parton densities assumed to be taken from existing parametrizations like GRV, MRS, CTEQ, etc.

The basic scale λ specifies the average transverse momentum carried by the quarks. The magnitude of λ can be fixed from the relation (3) between $\mathcal{F}^a(x, t)$'s and $F_1(t)$ form factor. The best agreement with experimental data [14] in the moderately large t region 1 GeV$^2 < |t| < 10$ GeV^2 is reached for $\lambda^2 = 0.7$ GeV^2 (see Fig.4). This value also gives a reasonable magnitude $\langle k_\perp^2 \rangle^u = (290\,\mathrm{MeV})^2$, $\langle k_\perp^2 \rangle^d = (250\,\mathrm{MeV})^2$ for the average transverse momentum of the valence u and d quarks in the proton. Similar models can be constructed for $F_2(t)$ and pion form factor $F_\pi(t)$ [15].
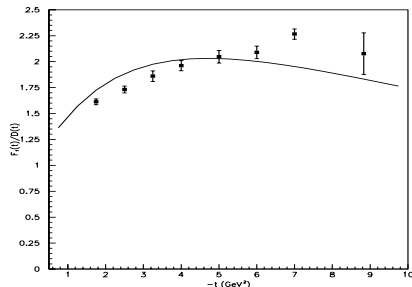
FIG. 4. Ratio $F_1^p(t)/D(t)$ of the $F_1^p(t)$ form factor to the dipole fit $D(t) = 1/(1 - t/0.71\,\mathrm{GeV}^2)^2$. Curve is based on the model having a Gaussian $k_\perp$-dependence (4) with $\lambda^2 = 0.7\,\mathrm{GeV}^2$.

It should be emphasized that the large-t real Compton scattering amplitude contains integrals with an extra $1/x$ factor. This results in a rather large enhancement of the Compton amplitude in the wide-angle regime. Keeping only the enhanced terms gives the WACS cross section as a product

$$\frac{d\sigma}{dt} \approx \frac{2\pi\alpha^2}{\tilde{s}^2} \left[\frac{(pq)}{(pq')} + \frac{(pq')}{(pq)} \right] R_1^2(t) , \tag{5}$$

of the Klein-Nishina cross section and the square of a new effective form factor $R_1(t)$. In the model of ref. [5], $R_1(t)$ is given by

$$R_1(t) = \sum_a e_a^2 \int_0^1 f_a(x) e^{\bar{x}t/4x\lambda^2} \frac{dx}{x} . \tag{6}$$

Comparison with existing data [16] is shown in Fig.5. Our curves follow the data pattern but are systematically lower by a factor of 2. Since we neglected several terms each capable of producing up to a 20% correction in the amplitude, we consider the agreement between our curves and the data as encouraging.

The angular dependence of our results for the combination $s^6(d\sigma/dt)$ is shown on Fig.5a. All the curves for initial photon ehergies 2,3,4,5 and 6

8

GeV intersect each other at $\theta_{\rm cm} \sim 60°$. This is in good agreement with experimental data of ref. [16] where the differential cross section at fixed cm angles was fitted also by powers of s: $d\sigma/dt \sim s^{-n(\theta)}$ with $n^{\exp}(60°) = 5.9 \pm 0.3$. Our curves correspond to $n^{\rm soft}(60°) \approx 6.1$ and $n^{\rm soft}(90°) \approx 6.7$ which also agrees with the experimental result $n^{\exp}(90°) = 7.1 \pm 0.4$.

This can be compared with the scaling behavior of the asymptotic hard contribution: modulo logarithms contained in the α_s factors, they have a universal angle-independent power $n^{\rm hard}(\theta) = 6$. For this reason, it is very important to perform precision measurements of $n(\theta)$ in future experiments at Jefferson Lab [17].
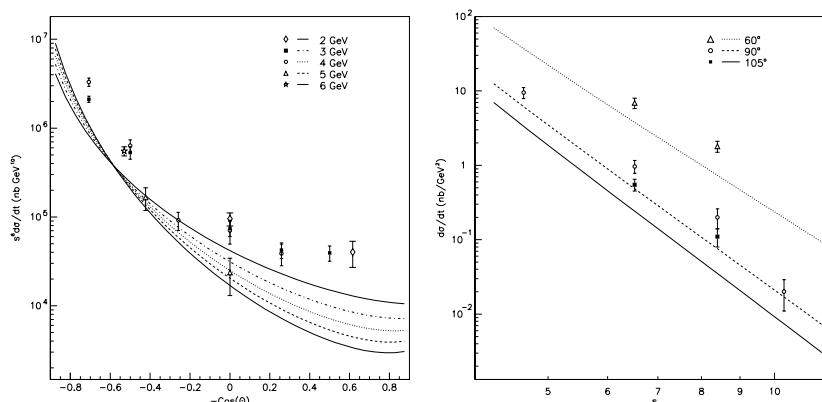

FIG. 5. a) Angular dependence of the combination $s^6(d\sigma/dt)$. b) s-dependence of the differential cross section $d\sigma/dt$ for $\theta = 60°$ (dotted line), $\theta = 90°$ (dashed line) and $\theta = 105°$ (solid line).

Above picture for the large-s, high-t behavior of the real Compton amplitude implies that the large-t behavior of the form factor type matrix elements is determined by an overlap of soft components of hadronic wave functions. It should be mentioned that for extremely large $|t| \gg 10\,{\rm GeV}^2$ this mechanism is subdominant. The dominant contribution is provided by hard gluon-exchange diagrams. There are all reasons to expect, however, that at accessible t the latter are negligibly small [5].

Conclusions. The hard exclusive electroproduction processes provide new information about hadronic structure accumulated in nonforward parton distributions. The NFPD's are universal hybrid functions having the properties of parton densities, hadronic form factors and distribution amplitudes. They give a unified description of various hard exclusive and inclusive reactions. The basic supplier of information about nonforward parton distributions is deeply virtual Compton scattering which offers a remarkable example of Bjorken scaling phenomena in exclusive processes. Wide-angle real Compton scattering is an ideal tool to test angle-dependent scaling laws characteristic for soft overlap mechanism. Hard meson electroproduction is the best candidate to see pQCD hard gluon exchange in exclusive reactions.

---

[1] X. Ji, Phys.Rev.Lett. **78** 610 (1997); Phys.Rev. D **55** (1997) 7114; J.Phys. G **24** (1998) 1181.
[2] A.V. Radyushkin, Phys. Lett. B **380** (1996) 417; Phys. Lett. B **385** (1996) 333; Phys. Rev. D **56** (1997) 5524.
[3] X. Ji and J. Osborne, hep-ph/9801260.
[4] J.C. Collins and A. Freund, hep-ph/9801262.
[5] A.V. Radyushkin, hep-ph/9803316.
[6] A.V. Radyushkin, hep-ph/9805342.
[7] V.Yu. Petrov et al. Phys.Rev. D **57** (1998) 4325.
[8] CLEO Collaboration (J. Gronberg et al.), Phys.Rev. D **57** (1998) 33.
[9] C.E. Hyde-Wright, these proceedings.
[10] J. C. Collins, L. Frankfurt and M. Strikman, Phys.Rev. D **56** (1997) 2982.
[11] L. Mankiewicz, G. Piller and T. Weigl, hep-ph/9711227.
[12] P.A.M. Guichon and M. Vanderhaeghen, Prog.Part.Nucl.Phys. **41** (1998) 125.
[13] M. Guidal, these proceedings and M. Vanderhaeghen, P.A.M. Guichon and M. Guidal, Phys.Rev.Lett. **80** (1998) 5064.
[14] L. Andivahis et al. Phys. Rev. D **50** (1994) 5491.
[15] A. Afanasev, these proceedings.
[16] M.A. Shupe, Phys.Rev. D **19** (1979) 1921.
[17] A.M. Nathan, these proceedings.